Optimizing Sensor and Human Inspection Network Layout for Time-invariant Health Monitoring of Locally Corroded Pipelines with High Confidence

Amin Aria*, Shapour Azarm, Mohammad Modarres

Center for Risk and Reliability
Department of Mechanical Engineering, University of Maryland, College Park, MD, 20742 USA

*Corresponding author: aaria@umd.edu

Abstract

Corrosion is one of the most common failure mechanisms in structures such as oil, gas and water pipelines. In particular, localized corrosion is difficult to monitor and can lead to structural failures, which may result in environmental damage, economic loss, and even human injury or death. To prevent corrosion failures, the extant literature reports on many Health Monitoring (HM) approaches. Sensor network design and human inspection planning are among the most popular HM schemes. In this paper, an optimization-based HM layout design approach for time-invariant monitoring of corrosion damages in pipelines is proposed. The key contribution in this paper is that a combination of a cost metric and HM reliability is optimized by simultaneously considering probability of detection, measurement error, and inference probability which determines the chance of a pipeline damage given the damage detected at some other part of the pipeline. The proposed method is demonstrated by two notional examples where uncertainties associated with sample data, such as damage size and intensity, are assumed to be known a priori, and then an optimized HM layout along a pipeline segment is determined. Two example with different problem sizes are used to illustrate applications of the proposed approach.

Keywords: Health monitoring, probabilistic damage detection, sensor network design, human inspection, optimization, corrosion

1. Introduction

Localized corrosion failure mechanisms are slow degradation processes that cause sparsely distributed damages. These mechanisms are difficult to detect, yet they are prominent in structures such as water, oil, and gas pipelines, bridges and railways, as shown, for example, by Lewandowski (2002) and Okeniyi et al. (2014). It is estimated that the global cost of corrosion is about 3.4% of global GDP, equivalent to US$2.5 trillion (NACE, 2016). All localized corrosion failure mechanisms (e.g., pitting and stress corrosion cracking) behave similarly (Chookah et al. 2011) and can be prevented using the same HM approach. Thus, a predictive HM approach, such as that proposed in this paper, tailored for a particular corrosion mechanism like pitting, can be used for other localized corrosion failure mechanisms and, in general, other similar slow degradation processes.

Abbreviations: AE: Acoustic Emission; HM: Health Monitoring; HI: Human Inspection; ILI: In-Line Inspection; IM: Information Metric; IP: Inference Probability; LPOND: Log-linearized Probability Of Not Detection; MVD: Modified Vulnerability Distribution; ME: Measurement Error; MINLP: Mixed Integer Nonlinear Programming; MST: Minimal Spanning Tree; PCI: Partial Coverage Inspection; POD: Probability Of Detection; POND: Probability Of Not Detection

This paper presents a new reliability-based HM optimization approach for pipelines subjected to internal corrosion. The objective of the approach is to minimize a combination of a measure of corrosion-based HM costs and a measure of detection of corrosion damages. A review of the literature on HM methods for pipelines, that are built upon condition-based maintenance rather than preventive and corrective maintenance (Rabiei et al., 2015), reveals that the approach developed in this paper is different from the extant literature in several ways, as discussed below.

(i) Among the most common data gathering schemes employed in the HM of pipelines are sensor network design, Human Inspection (HI) and In-Line Inspection (ILI) (Kishawy and Gabbar, 2010). These schemes are often considered separately in optimization models (Preis and Ostfeld, 2008; Guo et al., 2010; Sun et al., 2011; Gomes et al., 2013; Zhang and Zhou, 2014; Perumal, 2014; Alduraibi et al., 2016). However, stochastic nature of corrosion and implementation limitations of each of these schemes (Kishawy and Gabbar, 2010; Alaswad and Xiang, 2017) necessitate to consider a combination of them if having a flexible HM approach is desired. Furthermore, only a few key attributes of each of these schemes are considered in each of the extant models. For example, data acquisition frequency, data fidelity, sensor network configuration, coverage range, sensor type, and HM cost are among the key attributes of sensor network design. However, only some of them are considered in each of the available works (Marsh and Frangopol, 2007; Younis and Akkaya, 2008; Hart and Murray, 2010; Preis and Otsfeld, 2008; Zhu et al., 2011). On the other hand, for HI and ILI, labor costs, inspection locations, value of collected information, inspection quality and selection of an inspection tool are key attributes considered in the literature (Perumal, 2014; Zhang and Zhou, 2014; Vinod et al., 2016; Alaswad and Xiang, 2017). To more accurately and efficiently monitor the health of pipelines, the approach presented in this paper considers a combination of the above-mentioned schemes concurrently while their key attributes are modeled.

(ii) To measure and improve total (average) detection probability, various probabilistic detection metrics have been reported in the literature. Probability of Detection (POD) and probabilistic Measurement Error (ME) are two of these metrics (Rummel et al., 1974; Berens, 1989; Stephens and Nessim, 2006; Chatterjee and Modarres, 2013; Zhang and Zhou, 2014). Inference Probability (IP), defined as the probability of true prediction of the pipeline's state at a particular point given HM evidence at other points, is another detection metric which, to the best of our knowledge, has not been considered in the existing literature. Spatial variation of corrosion along a pipeline has been considered (De Leon and Macias, 2005; Zhou, 2010). However, IP as a probabilistic measure based on corrosion's spatial correlation has not been studied. Moreover, these probabilistic detection metrics are rarely considered in the context of optimization. As an example, Driessen et al (2017) have considered POD as a false negative probability in inspection optimization. In another study, optimal burn-in strategies are investigated while a Gaussian ME model is considered (Zhai et al., 2016). In the approach presented in this paper, the three aforementioned metrics are considered collectively in order to improve the detection probability.

(iii) Only a handful of previous works report on optimizing cost and detection probability concurrently (Younis and Akkaya, 2008; Shafiee and Sørensen, 2017). Detection probability (or integrity) is considered in some optimization-based maintenance studies (Chen et al., 2001; Zhang and Wicker, 2004; Xu et al., 2001; Gonzalez-Banos and Latomb, 2011) by using data fusion and increased redundancy (in terms of sensor coverage overlap) while the cost metric is minimized. However, as reported by Benstock et al. (2016), for Partial Coverage Inspection (PCI), increasing average detection probability by increasing redundancy is not necessarily a

cost-effective option for corrosion-based HM. Moreover, in the extant literature on optimal sensor placement, simplifying assumptions are used to mitigate the computational burden, especially when probabilistic HM metrics are considered. Popular simplifying assumptions include considering only one sensor type (Watson et al., 2004), modeling sensor network with a linear topology (Zhu et al., 2012), and network design with a pre-specified number of sensors (Hart and Murray, 2010). In contrast, the approach presented in this paper considers cost and detection probability concurrently while PCI, sensor network design and HI planning attributes are all considered with fewer simplifying assumptions.

In short, the approach proposed in this paper considers a cost-effective HM approach with high confidence for pipelines subjected to localized corrosion, while accounting for many factors that have been neglected in the extant literature.

The remainder of this paper is organized as follows. First, the overall problem statement and underlying assumptions are described in Section 2. Next, the steps of the proposed approach, including details of the detection metrics and optimization formulation, are provided in Section 3. Two notional examples including some results are presented in Section 4. The paper ends with some concluding remarks in Section 5.

2. Problem Statement

Consider a pipeline that is subjected to localized corrosion (Figure 1). It is assumed that, along the pipeline, data about the distribution of damages is known. The problem is to determine an HM layout for the pipeline. This layout includes the configuration (location and type) for all sensors and inspection tools to be used (e.g., by a human inspector) to acquire data regarding the state of corroded pipeline on its inner or outer surface (Figure 1). Note that this configuration layout of sensors on the surface of the pipeline is two-dimensional (2D). The layout is to be obtained by optimizing a weighted sum of an average detection probability and a cost metric.

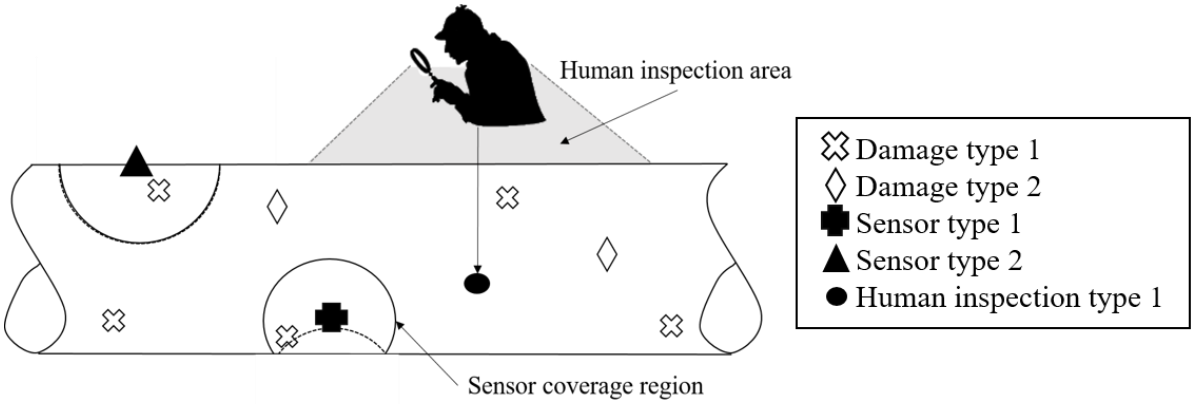

Figure 1- Schematic for pipeline HM problem

The key elements of the model for this problem are illustrated in Figure 2. An existing damage model is assumed to be available through prior analysis of historical data. This model indicates the growth behavior of damages, including probabilistic size of damages. Moreover, an existing pipeline vulnerability model in the form of distributions is assumed be known based on pipeline

monitoring history. These distributions essentially reveal the point-wise probability of having a damage of certain type and size at any arbitrary point on the inner surface of the pipeline.

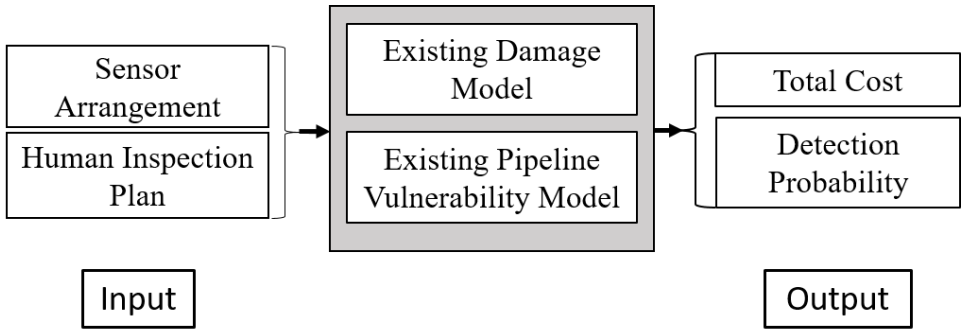

Figure 2- Key elements of the problem model

2.1 **Key Assumptions**

The key assumptions considered are:

i) Internal localized corrosion on the inner surface of the pipeline is assumed to be the only failure mechanism that causes damage. As such, all other failure mechanisms, pre-existing defects and flaws are not considered. However, the same approach can be used when external corrosion, or another similar failure mechanism, is considered.

ii) The proposed approach is static (time-invariant), which means the network configuration consists of nodes (potential locations of sensors) whose locations are based on spatial (not temporal) variation of damages.

iii) Considering the stochastic behavior of localized corrosion, a pipeline segment is defined as a part of a pipeline in which intensity (spatial density) of damages is constant.

iv) HI (which is a combination of a skilled inspector and an inspection tool) is modeled as a sensor with high coverage. This assumption also includes pigging of a pipeline. Sensors, HI, and ILI are all referred to as detection methods.

v) For a pipeline segment, the number of nodes is equal to the number of localized damages. Also, each damage can be detected by at most one sensor, since it is assumed that there is no coverage overlap among sensors. This assumption excludes HI.

vi) Each detection method has a circular area of coverage (Huang and Tseng, 2005), similar to a ‘binary disk’ sensing model (Zhu et al., 2012), with its center at the sensor node or inspection’s midpoint (the node where the HI is assigned to). This coverage circle is assumed to be placed on a 2D (unrolled) surface of the pipeline. The larger the radius of this circle, the higher the coverage capability of detection method.

vii) Underlying relations of IP matrices, which are discussed in detail in Section 3.3, are already known based on a pattern recognition technique and according to the history of damage data.

viii) All sensors are mounted on the exterior surface of the pipeline, even when they are used for internal corrosion monitoring as considered here.

3. Proposed Approach

The detection metrics, POD, ME, and IP, formulated and employed in the proposed approach are described in Sections 3.1-3.2. The steps of the proposed approach are detailed in Section 3.3. Finally, the optimization formulation is presented in Section 3.4.

3.1. Probability of Detection (POD)

POD is defined as the probability of detecting a damage by a sensor or by a non-destructive detection method. POD, in general, depends on several factors such as size and type of the damage, detection method used, and the distance between the damage and corresponding detection tool (e.g., sensor). These dependencies are typically investigated separately in the literature. For instance, dependency of POD on size (Zhang and Zhou, 2014) and damage to sensor distance (Pollock, 2007) are separately investigated for Acoustic Emission (AE) sensors. Here, a new aggregate model of POD as a function of size and damage to sensor distance is developed and used.

The use of the new aggregate POD model in the context of optimization is facilitated through a binary detection model, namely P_{exist}. This binary model indicates that a damage is detected by a particular detection method, regardless of its type and size, if and only if it is located in the coverage range of that detection method. The coverage range of a sensor is defined as the distance at which marginal POD of a damage with a random size is zero for that particular detection tool.

As shown in Figure 3, for an unrolled pipeline segment, the longitudinal and (unrolled) circumferential coordinates are used as the location of damages on the inner surface of the pipeline. To account for the circularity of the circumferential coordinate (y-axis in Figure 3), a replica of each damage, in addition to the original damage, is considered. The longitudinal component of the replica of a damage is the same as that of the original damage, and its circumferential component is $y\text{-}2\pi R$, where y denotes the circumferential component of the original damage and R is the internal radius of the pipeline. The origin of the proposed coordinates is located at the leftmost point of the bottom line of the pipeline. The location vector of both the damage and its replica are inserted into Eq. (1) (the P_{exist} model) to determine whether a damage is in the coverage range of the corresponding node (sc_j) or not. To do this, consider a damage k denoted by d_k (located at: $\mathbf{a}_k = (x_k, y_k)$) and damage i, d_i (located at: $\mathbf{a}_i = (x_i, y_i)$), as shown in Figure 3. Replicas of d_i (with location $\mathbf{a}_{i'} = (x_i, y_i\text{-}2\pi R)$) and d_k itself are in the coverage range of the sensor at node j (with the location at: $\mathbf{b}_j = (x_j, y_j)$). Hence, both damages are detected by the sensor at node j.

$$P_{exist}(d_i, s_j) = \begin{cases} 1 & \text{if } \|\mathbf{b}_j\text{-}\mathbf{a}_i\| \le sc_j \\ & \text{or } \|\mathbf{b}_j\text{-}\mathbf{a}_{i'}\| \le sc_j \\ 0 & \text{otherwise} \end{cases} \quad (1)$$

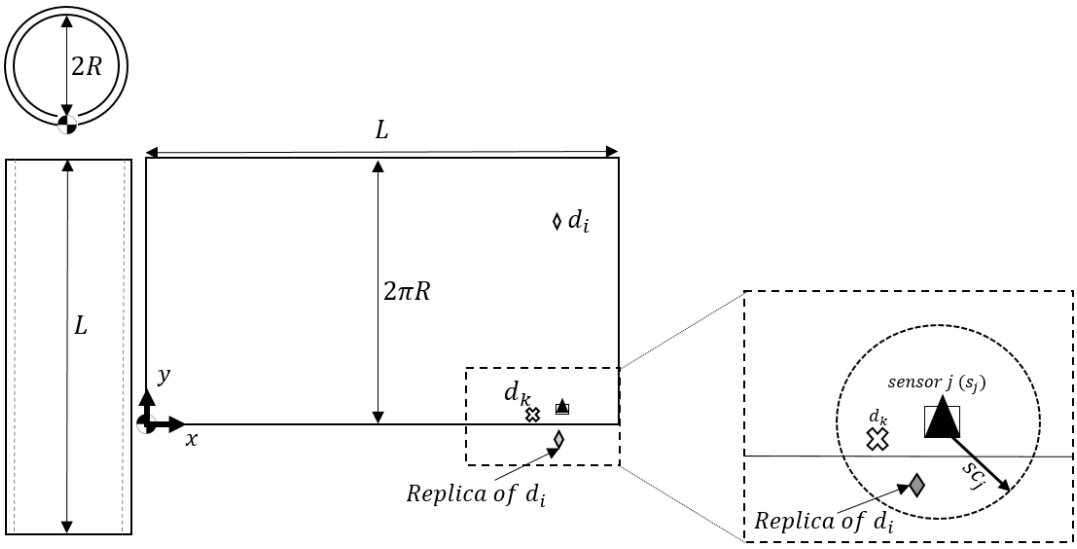

Figure 3- Geometry of damages on the inner surface for a pipeline segment

3.2 Inference Probability (IP)

IP is a detection metric that accounts for the probability of detecting a damage in the pipeline at a particular point (i.e., the likelihood of a damage of a given size and type at a particular location) given the HM data at some other point in the pipeline. The differences between IP and POD in the proposed approach are shown in Figure 4. As shown, a pipeline segment with two damage (shown with diamond and multiply symbols) and sensor types (triangle and plus symbols) are illustrated. A node is located in the vicinity of each of the damages, and detection methods are assigned to these nodes. For example, Sensor 4 is a type zero sensor (no sensor is assigned to its corresponding node).

Each sensor type has a specific coverage range, price, precision (ME), data acquisition frequency, and inference capability. In Figure 4, the coverage boundary is shown with dashed-double dot circles, while inference boundary is shown with dashed parabola-like curves. (Note that the second inference boundary of the sensor at node 1 (S_1) and sensor at node 3 (S_3) are not shown in the figure to avoid clutter.)

Inference boundaries are the locus of zero IP. In other words, $IP(s_j,d_i)$ corresponding to the sensor at node j (s_j) and damage i (d_i), will be zero at the inference boundary of node j. IP is a function of damage to node distance, detection method type, damage size and type, and similarity of affecting factors at damage and node locations. $IP(s_j,d_i)$ is unity if d_i is located at node j. On the other hand, a damage will be missed if IP values corresponding to all sensors in its vicinity are zero at the damage location.

If minimization of the probability of missing a true damage is desired, then sensors should be placed in a way that minimize POND, accordingly:

$$\Omega_i = (1-\Theta_i)\times(1-\Phi_i) = [\prod_{j=1}^{N}(\bar{\theta}_{i,j})]\times(1-\Phi_i) \qquad (2)$$

where Ω_i is POND of damage i, Θ_i is the aggregate IP of damage i (resultant IP of all detection methods assigned to nodes in the vicinity of damage i), and Φ_i is the aggregate POD of damage i (resultant POD of all detection methods assigned to nodes in the vicinity of damage i). $\overline{\Theta}$ is a matrix with row i for damage number and column j for node number, with its elements $\bar{\theta}_{i,j}$ for probability of missing damage i through inference based on HM data of the detection method used at node j. Note that in Eq. 2 (and elsewhere for the proposed approach), it is assumed that the probability of a false positive detection is zero.

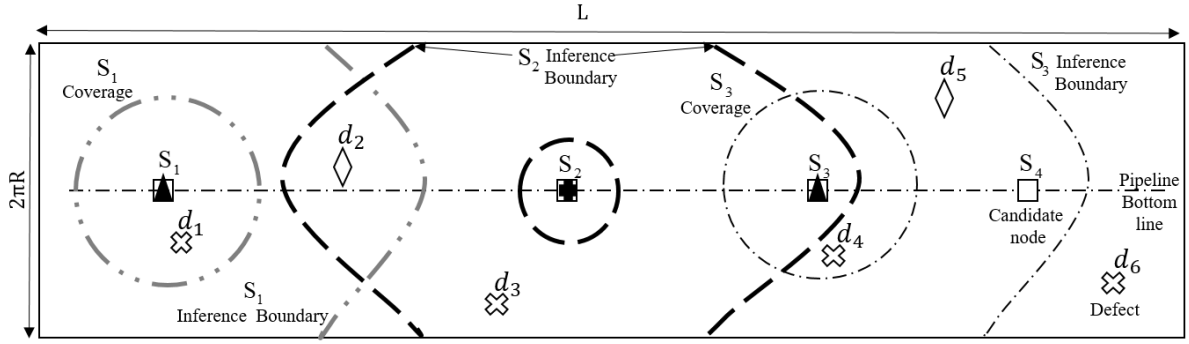

Figure 4- Coverage and inference boundaries along an unrolled pipeline of length L and inside radius R. Sensor nodes are located along the pipeline's bottom line (centerline of this figure) to facilitate illustration.

Since linearized equations are preferred in optimization, log-linearized POND, LPOND, is used:

$$\Omega'_i = [\sum_{j=1}^{N} \log(\bar{\theta}_{i,j})] + \log(1-\Phi_i) \quad (3)$$

where Ω'_i is LPOND of damage i.

3.3. Proposed Approach Steps

The steps of the proposed time-invariant HM approach are illustrated in Figure 5 .In this figure, numbers given to the right of the blocks refer to step numbers. These steps are detailed in the following.

Step 1 - Obtain Modified Vulnerability Distributions (MVDs): Prior maintenance and failure data of a similar pipeline are collected and analyzed to find the spatial intensity and size distribution of various damages in the pipeline. Data pre-processing, model selection, and model fitting are done in this step to obtain distributions. Corrosion failure risk analysis is also taken into account in the development of these distributions, which is why they are called "modified" distributions. In other words, the damages with higher risk of failure, considering corresponding failure consequences, are oversampled for modeling MVDs. Note that one modified size distribution is obtained for each of the damage types as a corresponding type-size MVD.

Step 2 - Determine Segments and Mesh Cell Size: Based on MVDs, the pipeline is segmented in such a way that the longitudinal spatial density of damages is approximately uniform for each pipeline segment. Each pipeline segment is then meshed into strips along its longitudinal direction. The only consideration in meshing is the cell size of the mesh. A cell is a strip with its width laid out along the longitudinal (x) axis of the pipeline. The size (width) of

each strip is to be small enough so that the probability of having more than one damage in each strip is negligible.

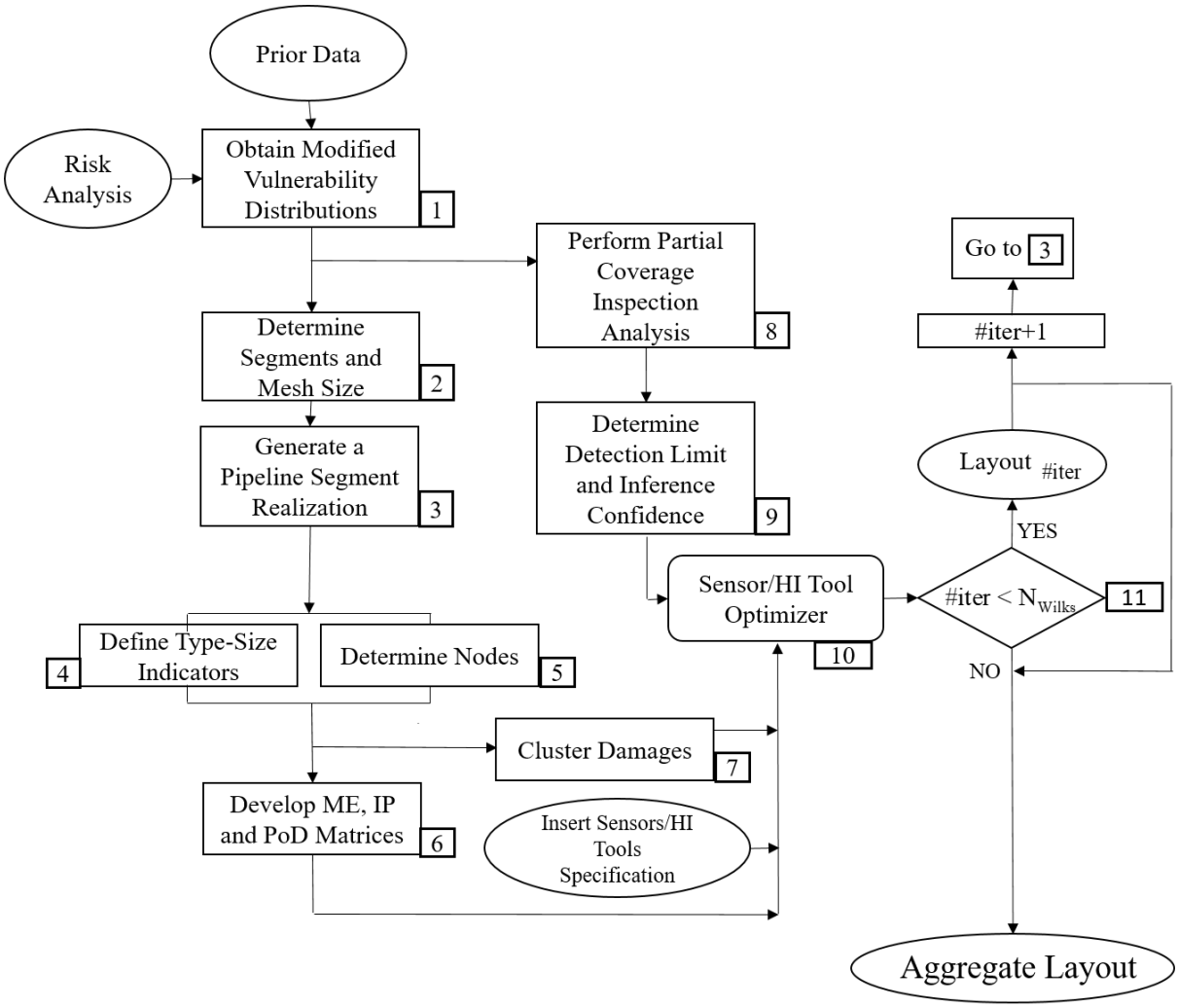

Figure 5-Schematic of the proposed static HM approach

Step 3 – Generate a Pipeline Segment Realization: Assuming a constant longitudinal density of damages along the segment, longitudinal MVD can be obtained using Poisson and binomial distributions (Chatterjee and Modarres, 2011). Subsequently, segment realizations, involving placement of damages with different size-types on strips, are determined. The Poisson distribution is used to calculate the probability of having a single damage of an arbitrary size-type in each strip. This value is used in a Bernoulli test as a success probability. If the simulated outcome of the Bernoulli test is one, damage is placed in the corresponding strip. (For non-uniform longitudinal damage density, refer to Valor et al. (2015))

The method presented above only considers longitudinal variations for the distribution of damages (Chatterjee and Modarres, 2011). However, it has been reported that the distribution of damages along pipeline circumference can be non-uniform. For example, in the case of "top of the line" corrosion in gas pipelines (Zhang et al., 2007), the probability of having a corrosion damage at the top half of a pipeline's cross section is higher than that at the bottom half. These kinds of variations can also be considered by extracting data points from a given circumferential damage distribution of the pipeline segment. The assumption here is that circumferential and longitudinal distributions of damages are independent.

Step 4 - Define Type-Size Indicators: Once a segment realization is simulated, a type-size class vector is determined for each of the damages of that realization. As mentioned earlier, one type-size MVD is developed for each damage type. Consequently, the types and sizes of damages are denoted here by the damage type-size classes. Each class refers to damages of a certain type, with their size corresponding to a particular interval. The size distribution is divided into classes of same cumulative probability, and Monte Carlo simulation is used to assign one of these classes to each of the damages. As an example, consider Figure 6 (Ossai et al., 2015), where a size distribution of pitting corrosion damages (type-size MVD) is shown. The number of classes is set to four. If a (randomly generated) class of damage i (d_i) is 3, d_i will be a pit with a depth in the interval 0.33-0.55 mm. Vector $\mathbf{C}_i$ (class vector corresponding to d_i) is a 0-1 vector where $\sum_{k=1}^{4} c_{i,k} = 1$. $c_{i,3}$ is unity for d_i since its size belongs to class 3.

This approach can also be used when multiple failure mechanisms (e.g., pitting corrosion and stress corrosion cracking) are considered. In that case, classes 1 to 4 may represent pitting corrosion size distribution, while classes 5 to 8 represent stress corrosion cracking size distribution.

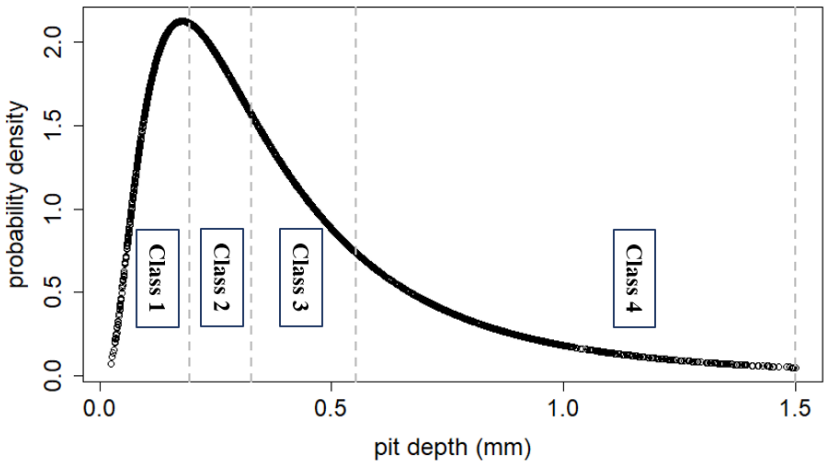

Figure 6- Example of type-size classes for depth (in mm) distribution of pitting corrosion damages

Step 5 - Determine Nodes: A single node is placed near each damage. The longitudinal location of a node is the same as that of the corresponding damage, while its circumferential location is different and is randomly generated to make it possible for the optimization solver to distinguish detection methods with different coverage capabilities.

Step 6 - Develop LPOND and POD Matrices: LPOND (Eq. 3) variations can be considered by developing ME, IP, and POD matrices. When damages' type-size classes are defined, an IP matrix will be formed for each combination of classes and detection methods with element $\overline{\theta^{k,m}}_{i,j} = 1 - \theta^{k,m}_{i,j}$ where k represents damage class and m represents type of detection method used. Then, in the optimization formulation, corresponding log-IP matrices will be used (Eq. 6.2) to calculate the IP term of Ω'_i (see Eq. 3).

It is necessary to assign a POD value to each possible damage-detection method combination to calculate the POD term of Eq. 3. Λ_i, a POD matrix of damage i, is developed to do so. Λ_i is a matrix whose $\lambda_{i_{m,j}}$ element corresponds to damage i of *a priori* known class k detected by

detection method type m (if used) at node j. In the development of Λ_i , it is assumed that POD of damage size and damage-node distance are fully independent, and there is no correlation between distance and size. Accordingly:

$$\lambda_{i_{m,j}} = \lambda^{s}_{i_{m,j}} \times \lambda^{d}_{i_{m,j}} \quad (4)$$

where $\lambda_{i_{m,j}}$ is an element of Λ_i , $\lambda^{s}_{i_{m,j}}$ is POD(size) for and $\lambda^{d}_{i_{m,j}}$ is POD(distance) of damage i and detection method type m at node j.

ME is an uncertainty metric defined as the difference between reported and true values of a quantity. ME is also modeled here using detection method and damage class vectors. To do this, matrix Δ is developed with rows corresponding to detection methods and columns corresponding to damage type-size classes. $\delta_{m,k}$ is the probability of the reported value of size of a damage of class k detected by detection method m being laid in the interval [(True size – ε_l), (True size + ε_u)]. The quantities ε_l and ε_u are the acceptable error margins, whose values are determined by experts. Δ'_j is the ME vector of node j. The mth element of this vector (δ'_{j_m}) corresponds to the detection of damage i=j, of *a priori* known class k, by sensor type m at node j. δ'_{j_m} is equal to probability of reported value of damage i=j being laid in the interval corresponding to the original type-size class when damage is detected by detection method m at node j. Vector Δ'_j is calculated using Eq. 5 where $\mathbf{C}_{i=j}$ is the type-size class vector for damage i that is located in the vicinity of node j .

$$\Delta'_j = \Delta \times \mathbf{C}_{i=j} \quad (5)$$

Note that $\delta'_{j,m}$ for HI at node j is set to be the mean ME value for all the damages in the corresponding inspection area.

Step 7 - Cluster Damages: Data clustering (or set partitioning) on a distribution of damages is conducted. Log-linearization employed in Eq. (3) leads to loss of sensitivity to changes in decimal probability values as long as the log-linearized equation considers only the order of magnitude of changes. To overcome this issue, damage clustering can be employed.

Clustering of damages distributed along a pipeline segment can be reduced to a Minimal Spanning Tree (MST) problem (Jain et al., 1999). However, inter-cluster distances are not considered in the MST problem. To consider the inter-cluster distances, a combination of MST and constrained k-means (Wagstaff et al., 2001) is developed here. In this clustering approach, the length of edges of the MST, with damages at its nodes, is determined. Next, the number of clusters is determined considering the length of MST edges and clustering distance limit. In general, wireless sensor energy consumption is an exponential function of its distance to the nearest sensor (Gue et al., 2010). Additionally, it is expected that inference accuracy will drop with distance, since it is assumed that adjacent locations are more similar in terms of corrosion behavior. Energy consumption and inference distance limits are defined considering these facts, and the minimum of these two limits is considered as the clustering distance limit. The number of clusters is determined considering this limit.

Knowing the number of clusters and clustering distance limit, the “cannot-link” damages, i.e., damages at the MST edges with their length greater than clustering distance limit, are defined for constrained k-means clustering where distance metric is defined based on Eq.1 and Eq. 6.9. The proposed clustering approach improves the distribution of detection methods as long as it helps with placing them proportional to the local density of damages.

Steps 8 and 9 - Perform PCI Analysis and Determine Detection Limit and Inference Confidence: PCI (Benstock and Cegla, 2016) is used to estimate the condition of the entire pipeline structure under study with minimum HM cost and a certain confidence level. PCI provides the coverage (damage detection) percentage required to obtain samples that include worst-case damages of the entire segment under investigation with P% confidence. The required detection percentage is used to define an overall detection constraint in the optimization formulation. It is also used to define a lower limit on detection for each damage cluster.

Step 10 – Performa Sensor/HI Layout Optimization: This step is described in Section 3.4

Step 11 - Wilks Method: To reduce the computational burden and account for stochastic nature of the localized corrosion in the simulation of pipelines, a modified Wilks method is used to capture existing variations in damages. The Wilks method (Wilks, 1941) is employed and modified by (Pourgol-Mohamad, 2007) to determine the minimum number of realizations of a random variable needed to capture at least p1% of the variations with p2% confidence. Steps 1 to 10 will be repeated N times, where N is number of realizations determined by the modified Wilks method. Consequently, N layouts will be attained and the final HM layout will be formed considering aggregation of these layouts.

The results from the pre-processing stage (steps 1 to 9) are fed into the optimization formulation (next section) to find an optimal detection arrangement with maximum average utility (minimum cost and maximum information value) and minimum average LPOND. A description of the optimization problem formulation follows.

3.4. Optimization Problem Formulation

The HM layout design problem is formulated as a single-objective optimization problem. The objective function (Eq. 6.1) is formed by a weighted sum of an average utility and an average LPOND function. The utility function is defined as a combination of the detection method's data gathering cost, coverage capability, data acquisition frequency, measurement error, and information value. The information value is a metric that quantifies the value of gathered data/information with respect to the reliability and amount of the acquired data/information. The utility will be maximized in order to maximize the information value and data acquisition frequency, while the cost of the HM set-up and ME are minimized. Note that an average LPOND is equivalent to the geometric mean of POND of all damages.

The constraints considered include (1) the detection limit (Eq. 6.15): this constraint is determined in the pre-processing stage using the PCI method. (2) The inference limit (Eq. 6.17): this constraint is also determined in the pre-processing stage. (3) Cost constraint (Eq. 6.19): the expected cost value of detection methods along a segment cannot be higher than a pre-specified limit.

In the proposed formulation, the detection method type vector is used to show the type of detection method used at each node. Each detection method is modeled with its specific coverage capability, precision (measurement error), cost, and information value. The detection method type zero represents assigning no sensor to the corresponding node. HI is also modeled as a high-coverage sensor (considering inspection tool and inspector's skill). It is also assumed that when HI is assigned to a node, the inspector will examine all the points in the inspection area that is centered at the HI node. Pigging can also be modeled as an HI with high information value, high cost, and high coverage.

The formulation of the optimization problem is given next, by Eqs. 6.1-6.21:

$$\underset{s_j}{\text{Minimize}}\left(w_1 \frac{E(\Omega')}{G_U} + (1\text{-}w_1)\frac{\text{-}U}{ub \times N} \right) \tag{6.1}$$

where:

$$\Omega'_i = \sum_{m=0}^{M}\sum_{j=1}^{J}\sum_{l=1}^{L}\sum_{k=1}^{K}\{\rho_j \times c_{i,k} \times id_{j,m} \times \log(\overline{\theta^{k,m}}_{i,j})\} + \sum_{j=1}^{N}\log\left(1\text{-}\eta_{i,j} \times \mathbf{C}_i^t \times \Lambda_i \times \mathbf{ID}_j\right) \tag{6.2}$$

$$U_j = w_{cost} \times U(cost_j) + U(IM_j) + w_{cov} \times U(cov_j) \tag{6.3}$$

$$IM_j = \sum_{m=0}^{M}[id_{j,m} \times (w_{Fr} \times Fr_m + w_{IV} \times IV_m - w_{ME} \times \delta'_{j,m}))] \tag{6.4}$$

$$\frac{\sum_{i=1}^{N}\Omega'_i}{N} = E(\Omega') \tag{6.5}$$

$$U = \sum_{j=1}^{N}(U_j \times (1\text{-}id_{j,1})) \tag{6.6}$$

$$0 \le w_1 \le 1 \tag{6.7}$$

Subject to:

$$\rho_j = 1 \text{, if } \sum_{i=1}^{N}\eta_{i,j} \ge 1 \text{, otherwise } \rho_j = 0 \tag{6.8}$$

$$\eta_{i,j}=1 \quad \text{if} \quad (x_i - x_j)^2 + \min(|y_i - y_j|, |t_i - |2\pi r - y_j||)^2 \le \mathbf{ID}_j.\mathbf{SC} \text{ , otherwise } \eta_{i,j}=1 \tag{6.9}$$

$c_{i,k}=1$ if damage at location i belongs to type-size class k, otherwise $c_{i,k}=0$ (6.10)

$$\sum_{k=1}^{Q} c_{i,k} = 1 \tag{6.11}$$

$id_{j,m}=1$ if $s_j = m$, otherwise $id_{j,m}=0$ (6.12)

$$\sum_{m=0}^{M} id_{j,m} = 1 \tag{6.13}$$

$$\pi_i = 1 \text{ , if } \sum_{j=1}^{N}\eta_{i,j} \ge 1 \text{ , otherwise } \pi_i = 0 \tag{6.14}$$

$$lb \times N \le \sum_{i=1}^{N}\pi_i \le ub \times N \tag{6.15}$$

$$s_j = \text{integer}, 0 \le s_j \le M \tag{6.16}$$

$$G_L \le \Omega'_i \le G_U \tag{6.17}$$

$$\sum_{j} \rho_j \geq uc_{ii}, j \in cluster_{ii} \quad (6.18)$$

$$E(cost_j) \leq co_u \quad (6.19)$$

$$Re_i = \sum_{j=1}^{N} \eta_{i,j} \leq Maxdet \quad (6.20)$$

$$\frac{\sum_{i=1}^{N} Re_i}{N} \leq Re_U \quad (6.21)$$

Eq. 6.2 represents LPOND$_i$ ρ_j (Eq. 6.8) is node usage indicator, and N is number of damages/nodes along the segment. $\eta_{i,j}$ (Eq. 6.9) represents the P_{exist} model where location of damage i is denoted by (x_i, y_i) and location of node j is denoted by (x_j , y_j). $\mathbf{C}_i$ is damage type-size vector with element $c_{i,k}$ (Eq. 6.10) ('t' superscript represents vector transpose). Each damage belongs to one and only one type-size class (Eq. 6.11), and Q is the number of classes. Λ_i is the POD matrix of d_i. $\mathbf{ID}_j$ is a vector whose m+1th element (Eq. 6.12-13) is equal to one if sensor type m is used at node j (Eq. 6.16) (M is number of available detection methods, including assignment of no sensor) . The first element of $\mathbf{ID}_j$ is 1 whenever sensor type zero (no sensor) is assigned to node j. **SC** is also a vector with its m+1th element equal to coverage radius of detection method type m. Lastly, the average LPOND ($E(\Omega')$) is calculated in Eq. 6.5.

Eq. 6.3 indicates the utility value corresponding to the detection method used at node j. $cost_j$ is the monetary cost of detection method s_j used at node j, cov_j is the coverage capability, and IM_j is the information metric of the same detection method. The utility of each attribute is given as input for each detection method. These values are subjective and should be determined by experts. For example, on a 0-1 scale, experts may decide that the cost utility of a sensor with 10 units cost is 0.9, while that of a sensor with 20 units cost is 0.3, and that of a sensor with 25 units cost is just 0.1. Total utility is defined by Eq. 6.6 where the utility of nodes with no sensor is assumed to be zero.

The information metric (Eq. 6.4) is defined as a linear function of data acquisition frequency (Fr_m), information value (IV_m), and ME associated with all damages detected by the detection method at that node. Weight factors, which are used in the calculation of information value, should be determined by experts.

The allowable range of objective function weight factor is defined in Eq. 6.7.

π_i is the overall detection indicator corresponding to damage i (Eq. 6.14) that is equal to one if damage i is detected through at least one detection method. Overall detection bounds, lb and ub (Eq. 6.15), are determined using PCI analysis. Also, LPOND of all damages along a segment should be in a range determined through PCI analysis and defined by G_L and G_U in Eq. 6.17

Eq. 6.18 defines the clusters. uc_{ii} is the minimum detection percentage for damages in cluster (ii). Furthermore, Eq. 6.19 defines an upper bound (co_u) on expected cost of the detection

method used at each node. Last, the redundancy of detection of each single damage should be smaller than an upper limit (Eq. 6.20). Average redundancy of detection should also be smaller than a limit (Eq. 6.21)

The objective function (Eq. 6.1) is a weighted sum of the normalized average LPOND and total utility. Note that the only design variables in this problem are s_j (Eq. 6.16), integer indicator of type of detection method used at node j. All other variables are either determined in the approach steps 1 to 9 or are a function of s_j.

The above mentioned optimization problem is solved using a Mixed Integer Non-Linear Programming (MINLP) (Bussieck and Pruessner, 2003) solver, since it involves non-linearity (Eq. 6.9) and there are both continuous (Eq. 6.9) and integer (Eq. 6.16) variables. Unfortunately, the well-known MINLP tool, BARON® (Tawarmalani and Sahinidis, 2005), cannot handle conditional type constraints. Hence, the (non-)linear equivalent of all such conditional constraints are formed. Moreover, the technique in (Crowder et al., 1983) is used to shrink the feasible region and thus help reduce the run-time.

Finally, using the optimization formulation, results are obtained for a number of different damage realizations determined using the Wilks method. The final solution (HM layout) is obtained by aggregating the results from all such realizations.

4. Examples

Two notional examples are solved in this section using the proposed approach. In the first example, Section 4.1, a short pipeline segment is solved to illustrate all steps of the proposed approach. To guarantee a 95% distribution coverage with 90% two-sided confidence, a minimum of 46 samples (realizations) of damages would be needed (Pourgol-Mohamad, 2007). Hence, the HM layout and trends corresponding to 46 realizations are discussed. A longer pipeline segment is considered in the second example, Section 4.2, where results corresponding to a single realization are presented. The only corrosion mechanism considered in both examples is internal pitting corrosion. The pit depth is considered as the damage size and the pit length is neglected since sensitivity analysis shows that depth is of more importance in reliability assessment of pipelines (Teixeira et al., 2008). For both examples, it is assumed that the pipeline segment under consideration is transporting oil. In the optimization formulation, for the first example, there are 142 continues variables, 198 binary variables, and 345 constraints. In the second example, which is a larger one, there are 490 continuous variables, 670 binary variables, and11,065 constraints.

4.1 Illustration Example

A pipeline segment of 50-m length (L) and 1-m radius (R) is considered. It is assumed that there are only two detection options: an AE sensor (detection method 1 (m=1)) and human inspection with an ultrasonic tool (detection method 2 (m=2)). Assigning no detection method to nodes is the other option (m=0). Table 1 shows the specifications assumed for detection methods.

4.1.1 Application of the proposed approach

The steps of the proposed approach for this example are as follows (see Figure 5).

Table 1- Values of specifications of HM options

Attribute	AE sensor	HI with ultrasonic tool
Coverage radius (m)	0.400	20.0
Cost	1.000	10.0
Utility (cost)	1.000	0.10
Utility (coverage)	0.013	1.00
Utility (frequency)	1.000	0.01
Utility (information value)	0.020	1.00

Step 1 - Considering the values reported in the literature (Wang et al., 2016; Lewandowski, 2002; Valor et al., 2015), it is assumed that the longitudinal internal pitting corrosion MVD of the segment under investigation is 0.2 damages per unit length of pipeline.

For circumferential variations of damage density, it is assumed that the oil pipeline under consideration is more likely to be corroded in the lower quadrant where water can accumulate and debris tends to deposit (Palmer-Jones et al., 2006). Hence, the circumferential intensity follows the normal distribution $N\left(\mu = 0, \sigma = \frac{3.14}{3}\right)$ with 0 along the bottom of the pipeline.

Step 2- Using Poisson distribution with identically, independently and uniformly distributed damages along the pipeline segment, the mesh strip width is found to be 0.5 meters so that the probability of having more than one damage at each mesh strips is less than 0.01.

Step 3 – Forty-six realizations of the segment under investigation are generated to guarantee capturing 95% of variations of location of damages with 90% confidence. The problem setup corresponding to the first realization is provided in Table 2.

Step 4 – Considering the size distribution presented in Figure 6, only four damage classes are considered and one class is assigned to each of twelve damages (Table 2) using Monte Carlo sampling. The resulting classes of damages are presented in Table 3. Attributes of each of damage classes , such as ME corresponding to damages of each class, if found through implementing the inverse transform sampling method.

Step 5- Twelve nodes, corresponding to twelve damages of the first realization, are located along the pipeline segment. Assuming no pipeline geometrical constraints exist, the longitudinal locations of the nodes are set to coincide with those of corresponding damages, while the circumferential location of the nodes is determined by adding a random value from the interval (-0.5, 0.5) to that of corresponding damage. This interval is chosen considering AE sensor coverage radius.

Table 2- Location of generated damages for the first realization

Damage #	Longitudinal Component (m)	Circumferential Component (m)
1	6.62	1.42
2	8.14	0.12
3	9.65	1.23
4	21.27	0.24
5	22.28	5.21
6	22.78	0.12
7	24.80	6.22
8	29.35	5.06
9	32.38	4.91
10	33.39	0.38
11	38.44	6.13
12	45.01	5.48

Table 3- Class of damages of the first realization

Damage #	1	2	3	4	5	6	7	8	9	10	11	12
Damage Class	4	1	3	1	2	2	4	4	3	4	2	1

Step 6- The ME probabilities for AE sensors and ultrasonic NDT tools are calculated using relations provided in (Rabiei and Modarres, 2013) and (Chatterjee and Modarres, 2013), respectively. The generated ME values are reported in Table 4 for different classes and detection methods.

Table 4- Class intervals and corresponding ME probabilities

Class #	ME for AE sensors	ME for HI with Ultrasonic	Class interval (mm)
1	0.013	0.14	[0 0.19]
2	0.060	0.15	[0.19 0.32]
3	0.045	0.14	[0.32 0.55]
4	0.015	0.14	[0.55 1.50]

Human error is not considered in the calculation of the ME probabilities of HI with the ultrasonic NDT tool. Nonetheless, it can be easily included as per (Drury and Watson, 2002).

Considering the information provided in (Pollock, 2007) for AE sensors, a decaying power relation is considered here as POD(distance), $\lambda^{d}_{i_{m=1,j}}$, (Eq. 7):

$$\lambda^{d}_{i_{m=1,j}} = 1 - 15.625 \times (\min(\|\mathbf{b}_j - \mathbf{a}_i\|, \|\mathbf{b}_j - \mathbf{a}_{i'}\|))^3 \quad (7)$$

POD(distance) for HI with ultrasonic ($\lambda^{d}_{i_{m=2,j}}$) is assumed to be 1 for all damages since the inspector brings the detection tool to the exact location of damage if it is in the inspection area.

On the other hand, POD(size), $\lambda^{s}_{i_{m,j}}$, is calculated for the AE and the HI with the ultrasonic NDT tool using distributions provided in (Zhang and Zhou, 2014) and (Chatterjee and Modarres, 2013), respectively. $\lambda^{s}_{i_{m,j}}$ is calculated for each of the four classes of damages in Figure 6, and the mean value corresponding to each class (Table 5) is used as $\lambda^{s}_{i_{m,j}}$ of damages in that class.

Table 5- POD(size) for different damage classes

Class #	$\lambda^{s}_{i_{m,j}}$ for Acoustic Emission	$\lambda^{s}_{i_{m,j}}$ for HI with Ultrasonic
1	0.32	0.02
2	0.54	0.07
3	0.72	0.25
4	0.90	0.77

Lastly, the IP matrices are developed. To find the pointwise correlation of corrosion damages along a pipeline segment, a pattern recognition practice on the segment under investigation should be carried out, and subsequently a similarity matrix should be obtained. This work should also be done for different time slices to see the correlation trend over time. However, due to a lack of real world data, it is assumed here that the only similarity metric to be considered is the distance. It is also assumed that correlation factors vary with the class of the damage and detection method type. Hence, four $\overline{\Theta}$ (1-IP, refer to Eq. 2) matrices are developed for four damage classes that may be detected by AE sensors. The underlying relation of each of these matrices is brought in Table 6. The maximum inference distance for all the relations is assumed to be approximately 20 meters. It is also assumed that this limit increases with size of the damage.

Table 6- Underlying relations of –log($\overline{\Theta}$) (1-IP) matrices for AE sensors

Damage class	Underlying relation for inference of damage i using sensor at node j
1	$\exp(\min(\|\mathbf{b}_j-\mathbf{a}_i\|,\|\mathbf{b}_j-\mathbf{a}_{i'}\|)/8.3-2.7)$
2	$\exp(\min(\|\mathbf{b}_j-\mathbf{a}_i\|,\|\mathbf{b}_j-\mathbf{a}_{i'}\|)/8-3)$
3	$\exp(\min(\|\mathbf{b}_j-\mathbf{a}_i\|,\|\mathbf{b}_j-\mathbf{a}_{i'}\|)/8-3.5)$
4	$\exp(\min(\|\mathbf{b}_j-\mathbf{a}_i\|,\|\mathbf{b}_j-\mathbf{a}_{i'}\|)/7-2.7)$

Since data gathered through HI, in comparison to a single AE sensor, reveals more comprehensive information on the condition of the entire pipeline segment, it is assumed that IP values corresponding to HI with ultrasonic are greater than and proportionate to those corresponding to the AE sensor. The proportion factor for -log($\overline{\Theta}$) of HI is assumed to be 1.5.

Step 7- A combination of MST, using Kruskal's MST algorithm (Kruskal, 1956), and K-means clustering, described in detail in Section 3.3, is used to cluster the damages of the first realization. Clustering distance limit is assumed to be 20 meters. Also, the minimum detection of each cluster (Table 7) is determined considering the PCI overall detection lower limit (Eq. 6.14).

Table 7- Clustered damages of realization #1

Cluster #	Damage #	Minimum Detection
1	1,2,3	1
2	4,5,6,7	2
3	8,9,10,11,12	2

Steps 8, 9- In parallel, it is assumed that the overall detection lower limit is found to be 50% for an estimation of the entire segment with 90% confidence. Considering the overall lower limit, minimum detection of each of clusters is determined in step 7.

Step 10- Subjective utility weights are used to form the utility function that is defined to be maximized. The weights are given in Table 8.

Table 8- Utility weights used in utility function

W_{cost}	W_{cov}	W_{FR}	W_{IV}	W_{ME}
0.3	0.3	0.1	0.15	0.15

The cost limit is set to be 24 for the first realization (see Table 1 for cost metric values). In other words, the HI can be assigned to at most two nodes of the corresponding layout. Also, LPOND limits (G_L and G_U in Eq. 6.17) are set to be 1.5 and 12.

4.1.2 Results and Discussion

The HM layout for the first realization is shown in Figure 7 where x is the longitudinal component of the rolled-out segment, y is the circumferential component (see Figure 3), and the objective function weight factor (Eq. 6.1) is set to be 0.5 . Figure 7 (a) corresponds to the case where clustering and ME are not considered. On the other hand, Figure 7 **(**b) corresponds to the case where damages are clustered and ME is considered.

In the HM layouts, stars represent nodes, while plus signs, asterisks, diamonds, and squares represent damages that belong to different classes. Dashed circles are the coverage boundary of the AE sensors, and shaded areas represent the inspection area. Double shaded areas are places that are inspected two times.

Dashed lines in Figure 7 (b) represent cluster boundaries. In both layouts a and b, there are 2 HI nodes and 4 AE sensors. Consequently, HM cost is the same for both layouts. However, the average detection redundancy is higher for layout b due to better distribution of sensors and HI nodes (Table 9). As expected, a comparison of features of these two layouts in Table 9 reveals that damage clustering has led to better assignment of detection methods, in terms of average utility and average detection redundancy, and significant reduction in run time.

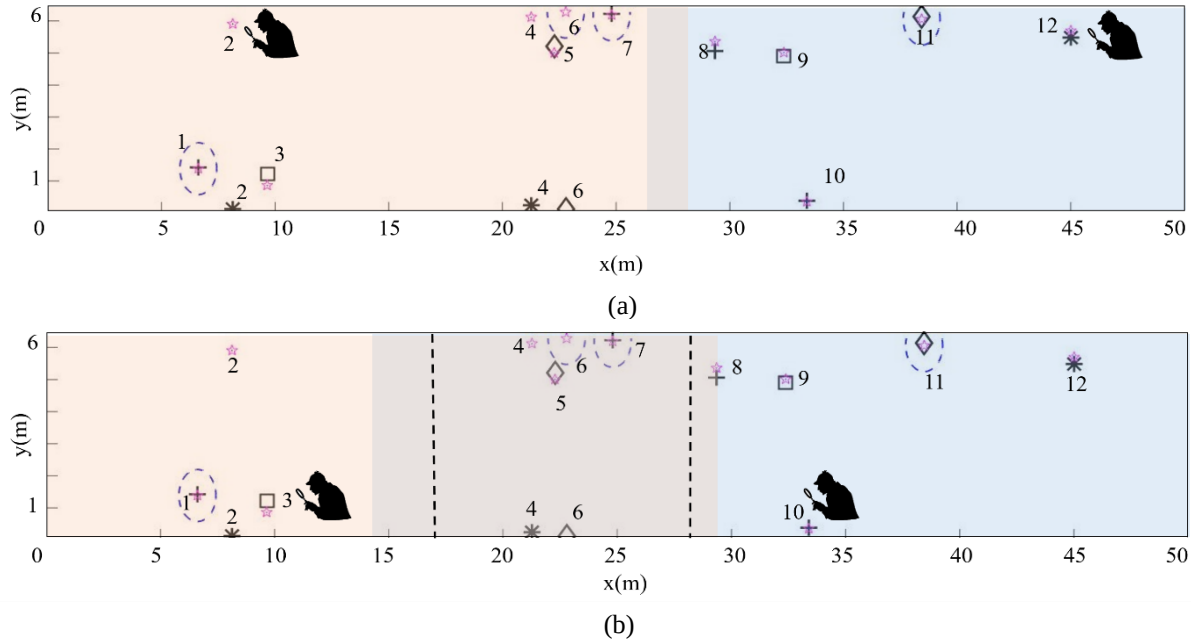

Figure 7- HM layout corresponding to first realization when (a) damage clustering and ME are not considered, (b) damage clustering and ME are considered

Table 9- Comparison of features of layouts corresponding to first realization

	Ave (Utility)	Ave (Redundancy)	Ave (-LPOND)	Run Time (s)
Without clustering and ME	0.31	1.33	9.78	106
With clustering and ME	0.50	1.5	10.10	93
Improvement %	61.29%	12.78%	3.27%	12.26%

The improvement in average utility and average -LPOND, when damage clustering and ME are considered, is indicated in Figure 8 for 46 realizations. It is shown that average utility per node and average redundancy per damage are improved for almost all the realizations. However, average -LPOND is slightly worse for some of the realizations when damage clustering and ME are considered. That is mainly due to more uniform distribution of detection methods considering local density of damages when clustering is utilized.

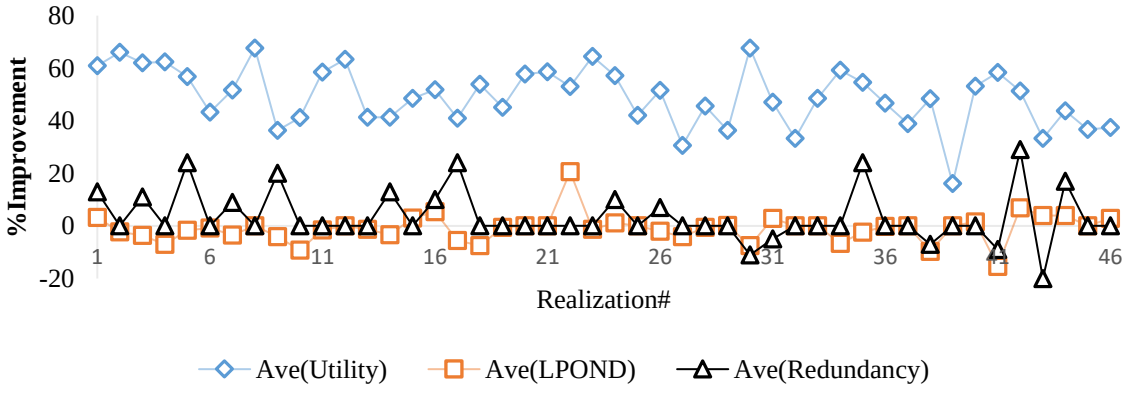

Figure 8- Improvement percentage when damage clustering and ME are considered

Improvement in run time when damage clustering and ME are considered is illustrated in Figure 9. As can be seen, run time drastically drops for almost all the realizations when damage clustering and ME are considered.

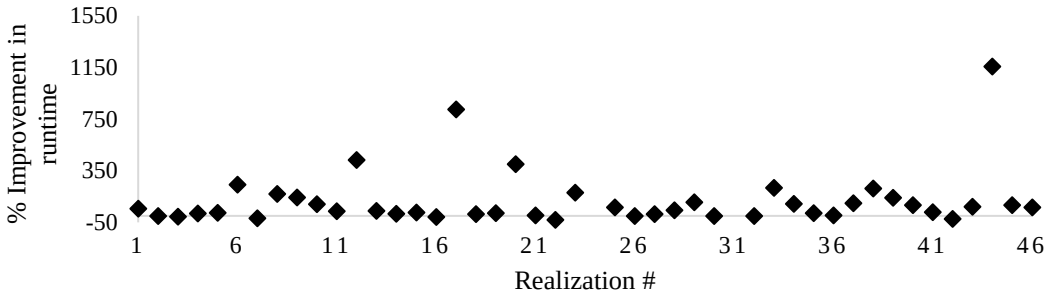

Figure 9- Improvement percentage in run time when damage clustering and ME are considered

To sum up, utilizing damage clustering reduces the run time by orders of magnitude, even for the more computationally complex case of layout with ME considered, with no concern of sub-optimality. Thus, the final layout of each realization should be the one that considers clustering and ME.

The scatter plot corresponding to aggregation of HM layout of all 46 realizations is depicted in Figure 10 where AE sensors are shown by triangles and HI with ultrasonic NDT tool is denoted by plus signs. As shown, the distribution of AE sensors and HI nodes is consistent with longitudinal and circumferential distribution of damages.

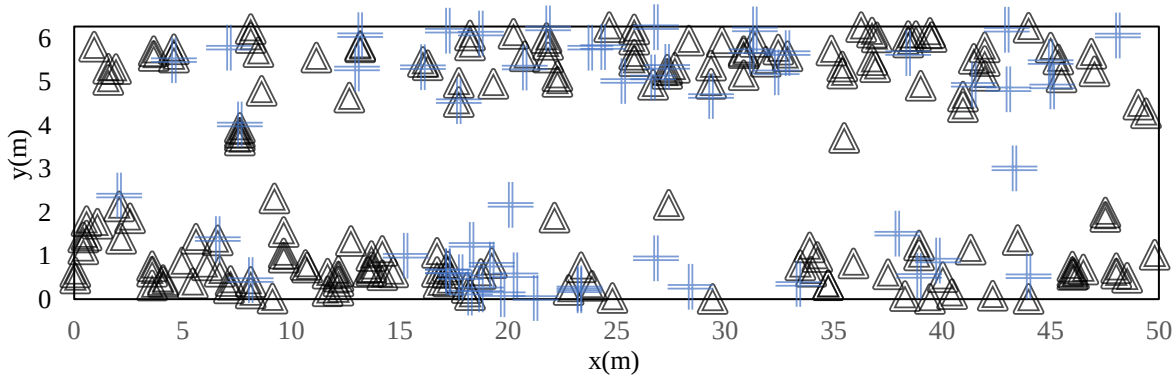

Figure 10- Scatter plot obtained through aggregation of all 46 HM layouts

There are 176 AE sensors and 54 HI nodes in Figure 10. As a result, it is expected that there will be 4 AE sensors and 1 HI with ultrasonic on average in each HM layout. Subsequently, the final static HM layout (Figure 11) is obtained where sensors and HIs are located at the center of 4 sensor clusters and 1 HI node cluster.

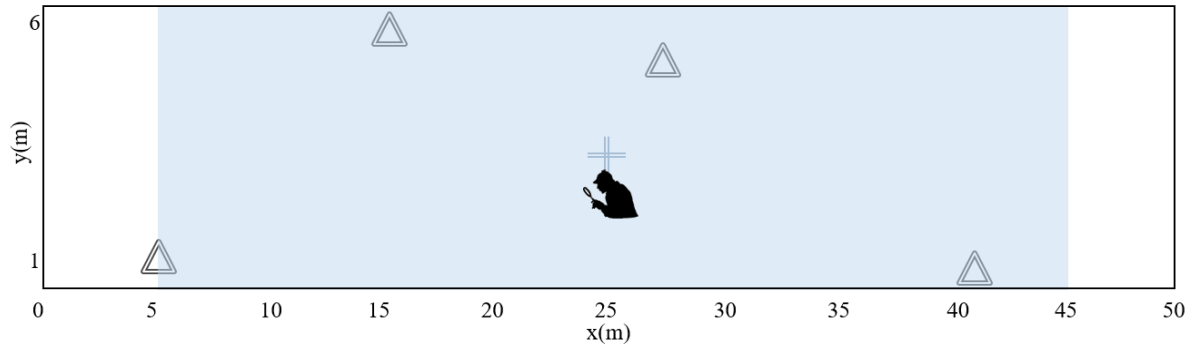

Figure 11- Final static HM layout corresponding to the pipeline segment under study

To verify the choice for a final static HM layout (Figure 11), performance of final the HM layout is compared with that of (Pareto) optimal designs corresponding to the most and the least expensive (in terms of HM total cost) layouts. Pareto optimal designs are different layout designs corresponding to various weight factors used in the objective functions (Eq. 6.1) of the HM design optimization problem.

In Figure 12, solutions represented by 31-1 through 31-4 and 45-1 through 45-2 are the longitudinal projection of Pareto designs corresponding to realizations 31 (most expensive layout) and 45 (least expensive layout), respectively. Triangles denote AE sensors while shaded strips denote inspection area. Double shaded strips represent regions which are inspected twice.

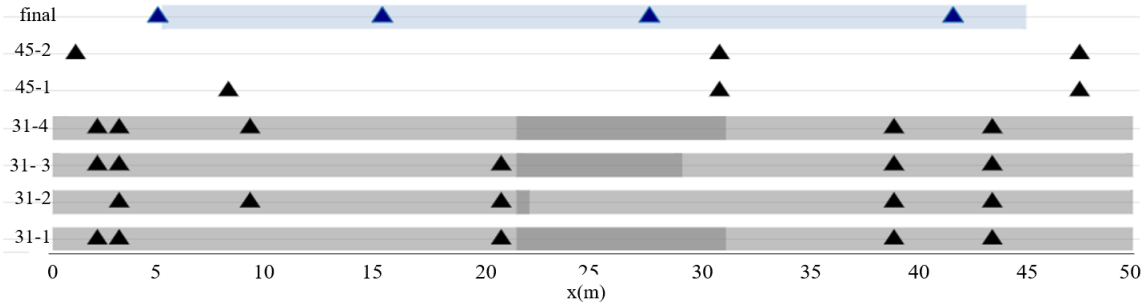

Figure 12- Longitudinal projection of final static HM layout and Pareto designs corresponding to most and least expensive layouts.

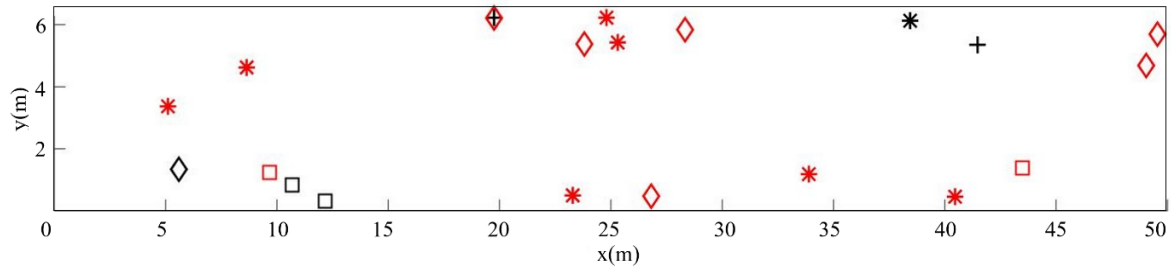

Figure 13- Two newly generated realizations used as test realizations

Using the Analytic Hierarchy Process (AHP) approach (Saaty, 1980), the performance of the layouts in Figure 12 was compared for two newly generated realizations of the segment under investigation (black and blue realizations in Figure 13). It turned out that the final static HM layout (Figure 11) outperforms all layouts of Figure 12 for both test realizations.

4.2 Longer Pipeline Example

In this example, a pipeline segment of 200 m length and 1 m radius is considered. It is assumed that longitudinal intensity of damage is 0.4 pit per unit length of the segment. All other assumptions, conditions, and relations used are the same as in the previous example.

The HM layout corresponding to one realization of the segment for this example is shown in Figure 14, where stars represent nodes, while plus signs, asterisks, diamonds, and squares represent damages that belong to different classes. Dashed circles are the coverage boundary of the AE sensors, and shaded areas represent the inspection area. Double shaded areas are places that are inspected two times.

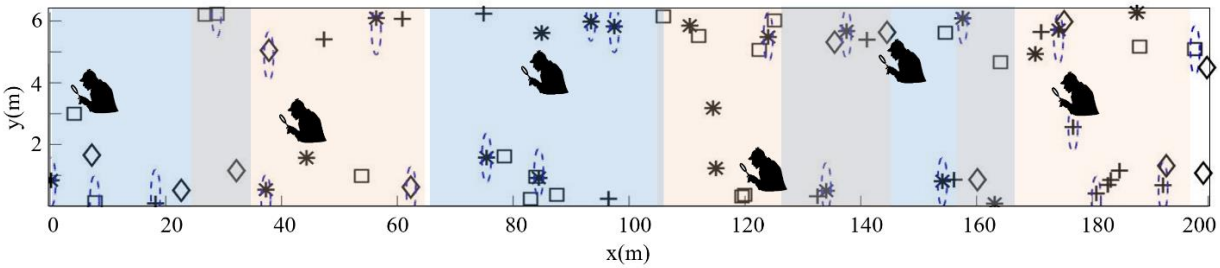

Figure 14- Static HM layout corresponding to one realization

5. Concluding Remarks

A new approach for obtaining HM layout for a pipeline segment subjected to internal pitting corrosion is provided. For this method, three detection metrics are considered simultaneously to improve the average detection probability corresponding to the optimal HM layout. In addition, the design of the HM layout is modeled as a single objective optimization problem where the objective is to optimize a weighted sum of a measure of corrosion-based HM costs and a measure of corrosion damage detection. The proposed approach considers information from human inspection in the HM layout alongside regular sensors. Moreover, a significant number of key attributes of detection methods are considered. In the approach, the partial coverage inspection is employed in order to improve the cost-effectiveness of the finalized HM layout, while the applicability of the proposed approach is improved by implementing damage clustering. Also, uncertainty associated with input sampling is considered using the Wilks method. The final output of the approach is an aggregated 2D HM layout that considers spatial distribution of different detection methods (including HI) along the pipeline segment.

6. Acknowledgements

This work was carried out as a part of the Pipeline System Integrity Management Project, which was supported by the Petroleum Institute, Khalifa University of Science and Technology, Abu Dhabi, UAE. This support is gratefully acknowledged.

7. References

Alaswad, S. and Xiang, Y., 2017. A review on condition-based maintenance optimization models for stochastically deteriorating system. Reliability Engineering & System Safety, 157, pp. 54-63.

Alduraibi, F., Lasla, N. and Younis, M., 2016, May. Coverage-based node placement optimization in wireless sensor network with linear topology. In Communications (ICC), 2016 IEEE International Conference on (pp. 1-6). IEEE.

Benstock, D. and Cegla, F., 2016. Sample selection for extreme value analysis of inspection data collected from corroded surfaces. Corrosion Science, 103, pp. 206-214.

Berens AP. 1989. NDE Reliability Data Analysis. In ASM Handbook, Volume 17: Nondestructive and Quality Control, pp. 689-701. ASM International, Materials Park, Ohio.

Bussieck, M.R. and Pruessner, A., 2003. Mixed-integer nonlinear programming. SIAG/OPT Newsletter: Views & News, 14(1), pp. 19-22.

Chatterjee, K. and Modarres, M., 2013. A probabilistic approach for estimating defect size and density considering detection uncertainties and measurement errors. Proceedings of the Institution of Mechanical Engineers, Part O: Journal of Risk and Reliability, 227(1), pp. 28-40.

Chen, B., Jamieson, K., Balakrishnan, H. and Morris, R., 2002. Span: An energy-efficient coordination algorithm for topology maintenance in ad hoc wireless networks. Wireless networks, 8(5), pp. 481-494.

Chookah, M., Nuhi, M. and Modarres, M., 2011. A probabilistic physics-of-failure model for prognostic health management of structures subject to pitting and corrosion-fatigue. Reliability Engineering & System Safety, 96(12), pp. 1601-1610.

Crowder, H., Johnson, E.L. and Padberg, M., 1983. Solving large-scale zero-one linear programming problems. Operations Research, 31(5), pp. 803-834.

De Leon, D. and Macías, O.F., 2005. Effect of spatial correlation on the failure probability of pipelines under corrosion. International journal of pressure vessels and piping, 82(2), pp. 123-128.

Driessen, J.P.C., Peng, H. and van Houtum, G.J., 2017. Maintenance optimization under non-constant probabilities of imperfect inspections. Reliability Engineering & System Safety, 165, pp. 115-123.

Drury, C.G. and Watson, J., 2002. Good practices in visual inspection. Human factors in aviation maintenance-phase nine, progress report, FAA/Human Factors in Aviation Maintenance, http://hfskyway.faa.gov.

Gomes, W.J., Beck, A.T. and Haukaas, T., 2013. Optimal inspection planning for onshore pipelines subject to external corrosion. Reliability Engineering & System Safety, 118, pp. 18-27.

González-Baños, H., 2001, June. A randomized art-gallery algorithm for sensor placement. In Proceedings of the seventeenth annual symposium on Computational geometry (pp. 232-240). ACM.

Guo, Y., Kong, F., Zhu, D., Tosun, A.Ş. and Deng, Q., 2010, April. Sensor placement for lifetime maximization in monitoring oil pipelines. In Proceedings of the 1st ACM/IEEE International Conference on Cyber-Physical Systems (pp. 61-68). ACM.

Hart, W.E. and Murray, R., 2010. Review of sensor placement strategies for contamination warning systems in drinking water distribution systems. Journal of Water Resources Planning and Management, 136(6), pp. 611-619.

Huang, C.F. and Tseng, Y.C., 2005. The coverage problem in a wireless sensor network. Mobile Networks and Applications, 10(4), pp. 519-528.

Jain, A.K., Murty, M.N. and Flynn, P.J., 1999. Data clustering: a review. ACM computing surveys (CSUR), 31(3), pp. 264-323.

Kishawy, H.A. and Gabbar, H.A., 2010. Review of pipeline integrity management practices. International Journal of Pressure Vessels and Piping, 87(7), pp. 373-380.

Koch, G., Varney, J., Thompson, N., Moghissi, O., Gould, M. and Payer, J., 2016. International measures of prevention, application, and economics of corrosion technologies study. NACE International IMPACT Report.

Kruskal, J.B., 1956. On the shortest spanning subtree of a graph and the traveling salesman problem. Proceedings of the American Mathematical society, 7(1), pp. 48-50.

Lewandowski, D., 2002. Gas pipelines corrosion data analysis and related topics, M.S. thesis, Delft University of Technology, Delft, The Netherlands.

Marsh, P.S. and Frangopol, D.M., 2007. Lifetime multiobjective optimization of cost and spacing of corrosion rate sensors embedded in a deteriorating reinforced concrete bridge deck. Journal of Structural Engineering, 133(6), pp. 777-787.

Okeniyi, J.O., Ambrose, I.J., Okpala, S.O., Omoniyi, O.M., Oladele, I.O., Loto, C.A. and Popoola, P.A.I., 2014. Probability density fittings of corrosion test-data: Implications on C6H15NO3 effectiveness on concrete steel-rebar corrosion. Sadhana, 39(3), pp. 731-764.

Ossai, C.I., Boswell, B. and Davies, I.J., 2015. Predictive modelling of internal pitting corrosion of aged non-piggable pipelines. Journal of The Electrochemical Society, 162(6), pp. C251-C259.

Palmer-Jones, R., Hopkins, P. and Eyre, D., 2006. Understanding the results of an intelligent pig inspection. Penspen Integrity, 8, pp. 1-16.

Perumal, K.E., 2014. Corrosion risk analysis, risk based inspection and a case study concerning a condensate pipeline. Procedia Engineering, 86, pp. 597-605.

Pollock, A., 2007. Probability of detection for acoustic emission. Journal of Acoustic Emission, 25, pp. 231-237.

Pourgol-Mohammad, M., 2007. Integrated methodology for thermal-hydraulics uncertainty analysis (IMTHUA) (Doctoral dissertation, University of Maryland, College Park).

Preis, A. and Ostfeld, A., 2008. Multiobjective contaminant sensor network design for water distribution systems. Journal of Water Resources Planning and Management, 134(4), pp. 366-377.

Rabiei, E., Droguett, E.L., Modarres, M. and Amiri, M., 2015. Damage precursor based structural health monitoring and damage prognosis framework. Safety and Reliability of Complex Engineered Systems, vol, pp. 2441-2449.

Rabiei, M. and Modarres, M., 2013. Quantitative methods for structural health management using in situ acoustic emission monitoring. International Journal of Fatigue, 49, pp. 81-89.

Rummel, W.D., Todd Jr, P.H., Frecska, S.A. and Rathke, R.A., 1974. The detection of fatigue cracks by nondestructive testing methods, Technical Report NASA CR 2369, National Aeronautics and Space Administration Martin Marietta Aerospace.

Saaty, T.L., 1980. Analytic Heirarchy Process. Wiley StatsRef: Statistics Reference Online.

Shafiee, M. and Sørensen, J.D., 2017. Maintenance Optimization and Inspection Planning of Wind Energy Assets: Models, Methods and Strategies. Reliability Engineering & System Safety, pp. 1-19.

Stephens, M. and Nessim, M.A., 2006. A comprehensive approach to corrosion management based on structural reliability method. Proceedings of IPC2006, ASME, Calgary, Paper No. IPC06-10458.

Sun, Z., Wang, P., Vuran, M.C., Al-Rodhaan, M.A., Al-Dhelaan, A.M. and Akyildiz, I.F., 2011. BorderSense: Border patrol through advanced wireless sensor networks. Ad Hoc Networks, 9(3), pp. 468-477.

Tawarmalani, M. and Sahinidis, N.V., 2005. A polyhedral branch-and-cut approach to global optimization. Mathematical Programming, 103(2), pp. 225-249.

Teixeira, A.P., Soares, C.G., Netto, T.A. and Estefen, S.F., 2008. Reliability of pipelines with corrosion defects. International Journal of Pressure Vessels and Piping, 85(4), pp. 228-237.

Valor, A., Alfonso, L., Caleyo, F., Vidal, J., Perez-Baruch, E. and Hallen, J.M., 2015. The negative binomial distribution as a model for external corrosion defect counts in buried pipelines. Corrosion Science, 101, pp. 114-131.

Vinod, G., Shrivastava, O.P., Saraf, R.K., Ghosh, A.K. and Kushwaha, H.S., 2006. Reliability analysis of pipelines carrying H2S for risk based inspection of heavy water plants. Reliability Engineering & System Safety, 91(2), pp. 163-170.

Wagstaff, K., Cardie, C., Rogers, S. and Schrödl, S., 2001, June. Constrained k-means clustering with background knowledge. In ICML (Vol. 1, pp. 577-584).

Wang, H., Yajima, A., Liang, R.Y. and Castaneda, H., 2016. Reliability-based temporal and spatial maintenance strategy for integrity management of corroded underground pipelines. Structure and Infrastructure Engineering, 12(10), pp. 1281-1294.

Watson, J.P., Greenberg, H.J. and Hart, W.E., 2004. A multiple-objective analysis of sensor placement optimization in water networks. In Critical Transitions in Water and Environmental Resources Management (pp. 1-10).

Wilks, S.S., 1941. Determination of sample sizes for setting tolerance limits. The Annals of Mathematical Statistics, 12(1), pp. 91-96.

Xu, Y., Heidemann, J. and Estrin, D., 2001, July. Geography-informed energy conservation for ad hoc routing. In Proceedings of the 7th annual international conference on Mobile computing and networking (pp. 70-84). ACM.

Younis, M. and Akkaya, K., 2008. Strategies and techniques for node placement in wireless sensor networks: A survey. Ad Hoc Networks, 6(4), pp. 621-655.

Zhai, Q., Ye, Z.S., Yang, J. and Zhao, Y., 2016. Measurement errors in degradation-based burn-in. Reliability Engineering & System Safety, 150, pp. 126-135.

Zhang, S. and Zhou, W., 2014. Cost-based optimal maintenance decisions for corroding natural gas pipelines based on stochastic degradation models. Engineering Structures, 74, pp. 74-85.

Zhang, X. and Wicker, S.B., 2004, April. How to distribute sensors in a random field? In Proceedings of the 3rd international symposium on Information processing in sensor networks (pp. 243-250). ACM.

Zhang, Z., Hinkson, D., Singer, M., Wang, H. and Nešić, S., 2007. A mechanistic model of top-of-the-line corrosion. Corrosion, 63(11), pp. 1051-1062.

Zhu, C., Zheng, C., Shu, L. and Han, G., 2012. A survey on coverage and connectivity issues in wireless sensor networks. Journal of Network and Computer Applications, 35(2), pp. 619-632.